Development and Control of a Hybrid Controlled Vertical Climbing Robot Based on Pneumatic Muscle Actuators

George Andrikopoulos[1], George Nikolakopoulos*[2], Stamatis Manesis[3]
[1,3]Electrical and Computer Engineering Department, University of Patras, Greece
*Control Systems and Interaction Division, Luleå University of Technology, Sweden
[1]andrikopg@ece.upatras.gr, *[2]george.nikolakopoulos@ltu.se, [3]stam.manesis@ece.upatras.gr

***Abstract*— This article presents the development and control of a novel hybrid controlled vertical climbing robot based on Pneumatic Muscle Actuators (PMAs). PMAs are highly non–linear pneumatic actuators where their elongation is proportional to the internal pressure. The vertical sliding of the robot is based on four PMAs and through the combined and sequential contraction–extension of the pneumatic muscles and cylinders, upward and downward movements are executed. For controlling the movement of the robot and to cope with the high non–linearities of the system, a simplified and highly functional hybrid control scheme, based on PID and On/Off control, has been adopted. The efficacy of the proposed scheme is presented through multiple experimental results where it is shown that the utilized controller is able to provide fast (on/off) and accurate (PID) translations to the robot.**

Keywords*— Pneumatic Muscle Actuator, Programmable Logic Controller, Climbing Robot, Switching Control, PID Controller

I. INTRODUCTION

Recently there has been a strong attention in the design and development of biologically inspired robots that will be able to move, run, climb and perform actions by mimicking the bio–structure and movement of animals, such as humans or insects.

More specifically, there has been a lot of research efforts in the areas of biomimetic robots that are designed to climb surfaces. Climbing robots can be used to perform several tasks such as inspection, observation, repair or act as communications relays. In [1], a climbing robot mechanism has been introduced which uses dynamic movements to climb between two parallel vertical walls by using a single actuated degree of freedom. Reference [2] proposes a wall climbing robot with permanent magnetic adhesion mechanism that is used for inspecting oil tanks. In [3] a climbing mobile robot has been developed for manufacturing and inspection applications within the aerospace industry. Reference [4] introduces a two DOF miniature cylindrical climbing robot with advanced mobility on ferromagnetic sheets. In [5], a bipedal climbing robot has been constructed using an under–actuated mechanism to minimize the number of motors and a hybrid navigation based motion planning method for autonomous control of the climbing robot. In [6] a miniature wall climbing robot has been designed with biomechanical suction cups actuated by Shape Memory Alloy (SMA) actuators.

Over the years, researchers have used various types of actuators on their robotic applications. Hydraulic, electric, magnetic and or pneumatic are some of the commonly utilized types, with respect to the application's characteristics, function and limitations. During the last decade, there has been an increase in the use of pneumatic actuators in Robotics due to their advantages such as low power to weight ratio, high strength and small weight.

Pneumatic Muscle Actuator [7], also known as the McKibben Pneumatic Artificial Muscle (PAM) [8], [9], [10], [11], Fluidic Muscle [12] or the Biomimetic Actuator [13], is a tube–like actuator that is characterized by a decrease in the actuating length when pressurized [14], [15], [16], [17], [18]. Best known member of this family is the McKibben–Muscle, which was invented in 1950s by the physician, Joseph L. McKibben and was used as an orthotic appliance for polio patients [8], while the first commercialization of PMAs has been done by the Bridgestone Rubber Company of Japan in the 1980s. PMAs are significantly light actuators that are characterized by smooth, accurate and fast response and also are able to produce a significant force when fully stretched.

Typical manufacturing of a PMA can be found as a long synthetic or natural rubber tube, wrapped inside man–made netting, such as Kevlar, at predetermined angle. Protective rubber coating surrounds the fibber wrapping and appropriate metal fittings are attached at each end. The PMA converts pneumatic power to pulling force and has many advantages over conventional pneumatic cylinders such as high force to weight ratio, variable installation possibilities, no mechanical parts, lower compressed–air consumption and low cost [19]. When compressed air is applied to the interior of the rubber tube, it contracts in length and expands radially. As the air exits the tube, the inner netting acts as a spring that restores the tube in its original form. This actuation reminds the operation of a single acting pneumatic cylinder with a spring return, while this reversible physical deformation during the contraction and expansion of the muscle results in linear motion. Typical types of PMAs and the corresponding naming are depicted in Fig. 1.An extensive overview of the most significant PMA applications can be found in [20].

The objective of this work is to design and implement a novel hybrid controlled vertical pneumatic climbing robot, based on PMAs. For controlling the vertical movement of this highly non–linear robot, a simplified and highly functional

hybrid control scheme has been adopted. The proposed hybrid scheme is based on: a) On/Off control for performing fast and not accurate reciprocative tensions displacements, and b) classical Proportional, Integral, Derivative (PID) control, for performing accurate displacements close to the a priori selected set–point.

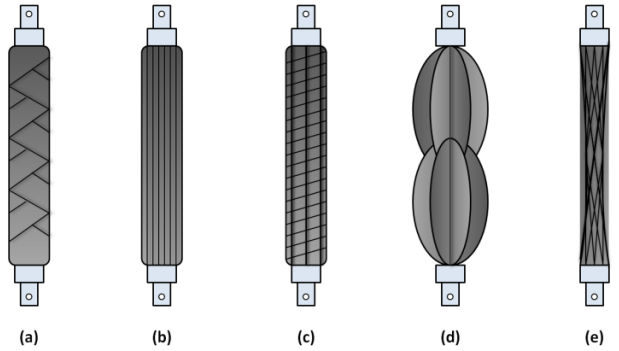

Fig. 1 Various types of PMAs: (a) McKibben Muscle/Braided Muscle, (b) Pleated Muscle, (c) Yarlott Netted Muscle, (d) ROMAC Muscle and (e) Paynter Hyperboloid Muscle.

The main novelty of this article is the construction of the climbing robot, based on the PMAs and the establishment of a hybrid control scheme that will allow the robot to climb by mimicking the movements that a human executes when climbing a ladder. It is worth to mention that based to the author knowledge, this is the first time in the scientific literature that such a robotic climber, has been developed and controlled based on PMAs.

This article is structured as follows. In Section 3 the simplified modeling of the vertical climbing actuator is being presented, followed by the development of the PID control scheme. In Section 2 the development of the hybrid controlled robotic climber is presented while in Section 4, experimental results that prove the efficacy of the proposed scheme are depicted. In the last Section 5 the conclusions are drawn.

II. MODELING& CONTROL OF THE CLIMBING ROBOT

The structure and the movements of the proposed robotic climber are based on four PMAs. The PMAs are actuators that are very similar to the skeletal muscle behaviours as far as it is concerning the speed and the applicable force that can generate.

Various modeling approaches have been presented in the scientific field of PMA modeling. These models although incorporate basic and more detailed analysis of PMAs, in the area of PMA applications, most of the models are based on the geometry of the PMA, mainly due to the model's simplicity and great relativity to the experimental behaviour. An extensive overview of the most significant PMAmodels can be found in [21].

Among these models, the Tondu and Lopez model [22] has been widely utilized in most PMA applications. In this case, the model of the PMA is derived based on the hypothesis that the actuator is consisted of a cylindrical shaped muscle that takes a conic shape at both ends when it contracts. The generated force can be defined as:

$$F(\varepsilon, P) = (\pi r_0^2)P[\alpha(1-k\varepsilon)^2 - \beta], \quad 0 \le \varepsilon \le \varepsilon_{max} \tag{1}$$

where $\varepsilon = (l_0 - l)/l_0$ and $\alpha = 3/tan^2(\alpha_0), \beta = 1/sin^2(\alpha_0)$ and the following definitions: P is the control pressure, ε is the contraction ratio, $\alpha_0$is the initial braid angle, l_0 and l are the initial (unpressured) and the current length of the PMA respectively and k is a parameter for adapting theoretical value of the contraction ratio to the real experimental PMA and usually takes values $k \le 1$. Moreover the maximum contraction ratio can be defined as:

$$\varepsilon_{max} = (1/k)(1 - \sqrt{\beta/\alpha})$$

For the robotic climber, as the one presented in Fig. 2, during its movement the applied forces, are the PMA forcesF_i $(i = 1,2,3,4)$, the friction$T$ and the weight $mg$of the robot.

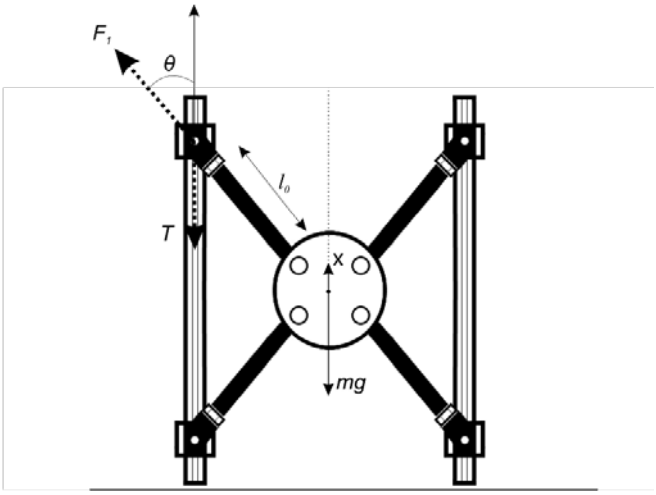

Fig. 2 The vertical climbing robot prototype

For small deviations Δx of the robotic climber's center of gravity, the deviation of the PMA's length can be defined as:

$$l = l_0 - \frac{\Delta x}{cos(\theta + \Delta\theta)} \tag{2}$$

Based on the assumptions that: a) the body of the robotic climber is symmetrical, b) the structure is rigid, c) the center of gravity and the body fixed frame coordinate system coincide, d) the torsional forces produced by the PMAs, at the robotic joints with the sliders, are very small and can be omitted, e) the four PMAs are defined by the same non—linear equation, and f) the upper body and the lower body of the robot are not operated at the same time instant, the vertical translation of the robotic climber can be defined as:

$$2Fcos(\theta + \Delta\theta) - 2T - mg = m\Delta\ddot{x}$$

where m is the total mass of the robotic climber and T is the friction forces, assumed to be the same at all the points of contacts with the climbers joints, defined as:$T = \eta F \sin(\varphi)$, and with a friction factor $\eta \in (0.1 - 0.25)$. By combining equations (1-2) the general nonlinear dynamics for the climber (based only on the upper robotic hands) can be defined as:

$$2(\pi r_0^2)P\left[\alpha\left(1 - k\left(\frac{\Delta x}{l_0\, cos(\theta + \Delta\theta)}\right)\right)^2 - \beta\right] cos(\theta + \Delta\theta) - 2T - mg = m\Delta\ddot{x} \quad (3)$$

The hybrid control scheme is based on a combination of: a) On/Off control, and b) PID control loop. The On/Off control is utilized only for the fast and not accurate climbing of the robot, while the PID control is energized when the robot is approaching the a priori defined set–point and for achieving maximum accuracy. By considering a $T_s \in \mathbb{R}^+$sampling time, and by defining $u(kT_s) \in \mathbb{R}$ the control action at the $k \in \mathbb{Z}^+$time instant, the transfer functions for the On/Off and PID controllers are presented in the following equations (4) and (5) respectively.

$$u_{On/Off} = \begin{cases} u^{max}, & e \geq 0 \\ u^{min}, & e < 0 \end{cases} \quad (4)$$

$$u_{PID} = K_p + \frac{K_i T_s}{2}\frac{1 + z^{-1}}{1 - z^{-1}} + \frac{K_d}{T_s}(1 - z^{-1}) \quad (5)$$

where$u^{max}, u^{min} \in \mathbb{R}$are the a priori set bounds for the On/Off controller, e is the tracking error, $K_{p,}K_i$, $K_{d,}$ are the PID controller's gains, and z^{-1} is the delay operator. The block diagram of this hybrid control scheme is presented in Fig. 3.

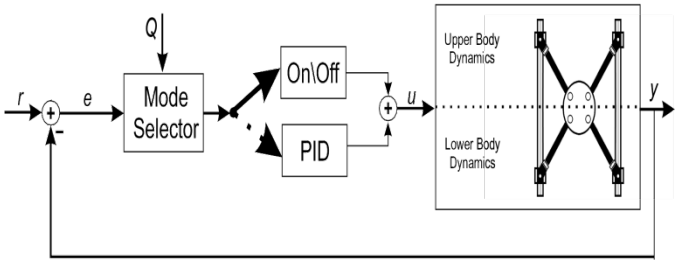

Fig. 3The proposed hybrid control scheme

In the proposed hybrid control scheme, the mode selector is the function block that rules the switchings among the On/Off and the PID control actions. The operation of the mode selector is based on a priori selected tolerance $Q \in \mathbb{Z}^+$. When the tracking error is $e \in (Q, -Q)$, the PID controller is being selected, otherwise the controller is based on On/Off. The Q factor represents a trade off between accuracy and speed of convergence as the selection of high tolerance values, result in slower and higly accurate responses, while the selection of lower tolerance values, result in faster and less accurate responses.

In the proposed control scheme and in order to avoid rapid oscillations around the set–point, a deadband for the PID controller has been utilized. For avoiding dangerous overshoots of the robotic climber vertical movement, constraints have been set to both control actions. These state and input constraints are formulated by utilizing a set of Hizeroed 2×4 matrices except for their$i$–th column which is equal to$[1, -1]^T$. More specifically, for each of the individual subsystems on the basis of which the controller is constructed, the constraints are formulated as follows:

$$\begin{bmatrix} H_1 \\ H_2 \\ H_3 \\ H_4 \end{bmatrix}_{8x4} \cdot \begin{bmatrix} x \\ \theta \\ u_{On/Off} \\ u_{PID} \end{bmatrix}_{4x1} \leq \begin{bmatrix} 600\text{mm} \\ 2400\text{mm} \\ 45^o \\ 60^o \\ 1\text{bar} \\ 5\text{bar} \\ 0.3\text{bar} \\ 5\text{bar} \end{bmatrix}_{8x1} \quad (6)$$

Where Hiis being defined as:

$$H_i = \begin{bmatrix} 0_{2\times i-1} & \underbrace{\begin{matrix} 1 \\ -1 \end{matrix}}_{i-column} & 0_{2\times 4-i} \end{bmatrix}_{2x4}$$

III. THE VERTICAL CLIMBING ROBOT

The experimental robotic climber, depicted in Fig. 4, consists of four pneumatic artificial muscles. The one end of each muscle respectively is attached to a common platform that plays the role of the mechanical climber's body, while the other end is attached to a sliding mechanism, which allows the movement of the robot, across the surface of the aluminium beams that form the vertical climbing platform. A small pneumatic cylinder is also attached to every sliding mechanism and it is utilizing compressed air to drive the sliding of the corresponding PMA to a halt. The climbing robot consists of two vertical aluminium beams of 3m in length and 40mm in width, which are placed at a distance of 40cm from each other. The mechanical climber consists of four Festo DSMP-20-305N-AM-CM Fluidic Muscles. Proportional pressure regulators, regulate the supply and pressure of that compressed air. For the experimental setup four Festo VPPM-6F-L-1-F-0L6H-V1N Proportional Pressure Regulators have been utilized, one for every corresponding muscle. The VPPM regulator has been designed to regulate a pressure proportional to a specified set-point value. An integrated pressure sensor records the pressure at the working line and compares this value to the set-point value. In the case of deviations between the set-point and actual value, the regulator is actuated until the output pressure has reached the set-point value. The measurement of the climber's center of gravity is achieved by an ASM WS12 cable actuated linear position sensor.

A pneumatic cylinder is attached to each one of the four sliding mechanisms (Fig. 5). The type of cylinders used is single acting with spring return. Four CEME 2/2 Way Normally Closed Digital Pressure Regulators control the pressure of the compressed air that is supplied to the

corresponding pneumatic cylinders. These cylinders play the role of the brakes and bring the movement of the mechanical climber's limbs to a halt. The brake's operation follows the On/Off philosophy. With no air supply, the brake is turned off, enabling the movement of the corresponding limb. With maximum air supply (6bar) the brake is activated and causes the halt of the limb's movement.

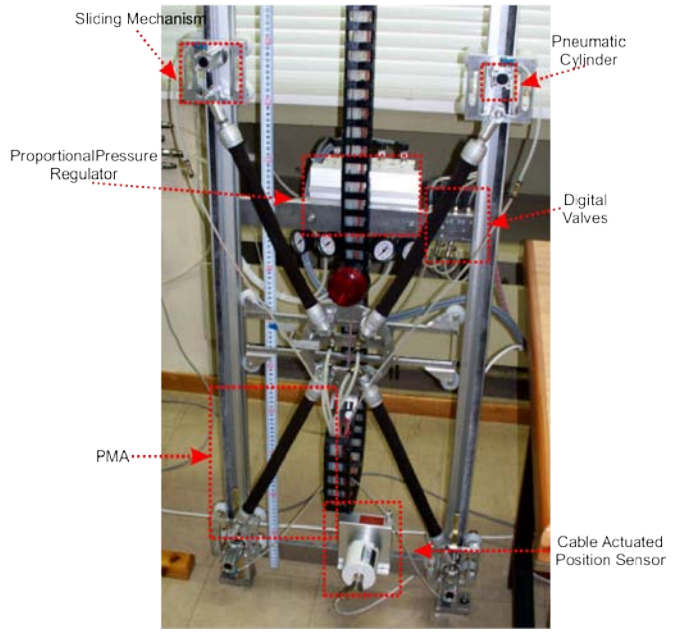

Fig. 4 The vertical climber robot prototype

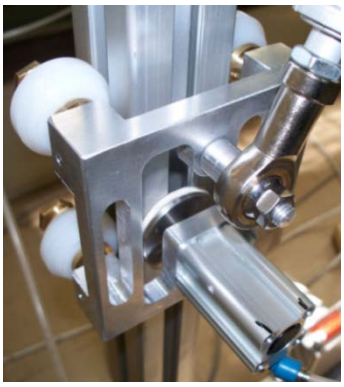

Fig. 5 The slider mechanism

The sequential On/Off and PID control actions as also the corresponding control sequence for the PMAs for achieving the vertical translation of the robotic climber are depicted in Fig. 6, where all the modes of operation and the relative transitions among the operational modes are also being highlighted.

The robotic climber's movement initiates with the execution of the On/Off control actions on the PMAs. While in idle state, the robot has all its brakes enabled, and all its muscles extended. The ascent begins when the lower brakes are being disabled and then the lower and upper muscles contract. In the sequence, the lower brakes are being enabled and the upper ones disabled which leads to the extent of the upper muscles. The next step is to disable the lower brakes so it can be possible for the lower muscles to extent. Finally, with the enable of the upper muscles the robot returns to the idle state, after accomplishing a vertical step movement.

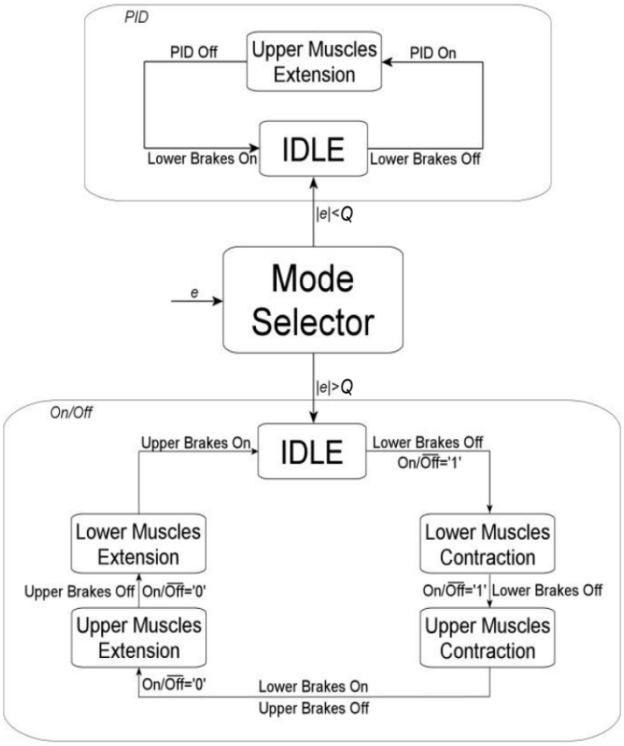

Fig. 6 Operational state diagram of the robotic climber

The PID position control algorithm is enabled when the difference between the climber's height and the desired final position e, becomes smaller than the predetermined tolerance area Q. Initially, the robot's lower brakes are disabled and the PID control is enabled causing the upper muscles to contract or extend according to the increase or decrease of the air pressure respectively. This operation is also causing a shift in the climber's position, while the PID control action ends when the pressure of the upper muscles reaches a specific value that can cause such a shift of position that brings the climber to the desired height.

IV. EXPERIMENTAL RESULTS

For the first experimental test–case, the gains of the PID controller have been set to $K_p = 20, K_i = 0.04, K_d = 0.01$,the deadband has been set to3 mm, while the reference altitude for the robotic climber has been set to 1000 mm. The response of the system is depicted in Fig. 7 where it is shown that in the first climbing stage of the robot, the On/Off controller executes sequential step ups of the climber by combining sequential contraction–extension of the pneumatic muscles and cylinders. When the height of the climber is being inserted in the a priori defined tolerance area Q (in this case $|e| \leq 10$), the control scheme is altered to PID and the climber manages to track the defined set-point.

In the second experimental test–case, the gains of the PID controller have been set to $K_p = 40, K_i = 0.18, K_d = 0.01$,the deadband has been set 3mm, while the reference altitude for the robotic climber has been set to 1400mm,. For this case, the

response of the system is depicted in Fig. 8 where it is shown the same behaviour in the climbing pattern, where the On/Off controller is initially activated until the height of the climber reaches is being inserted in the a priori defined tolerance area Q (in this case $|e| \leq 20$), and the control scheme is again altered to PID.

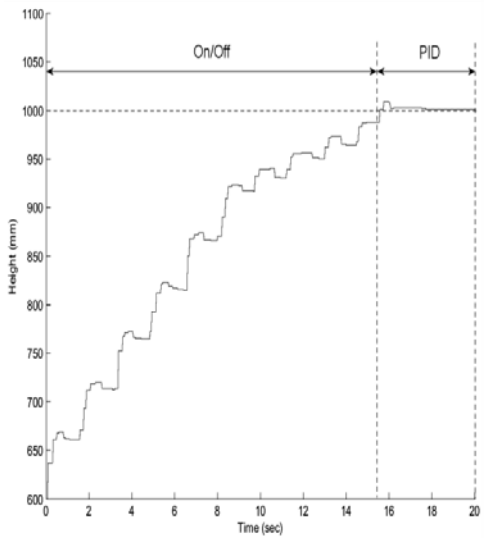

Fig. 7 Robotic climber experimental response ($r = 1000$ mm, $K_p = 20, K_i = 0.04, K_d = 0.01, Q = 10$)

Based on multiple executed experimental test–cases, it should be noted that by retaining the proportional gain to the value of $K_p = 60$, with a significant increase in the K_i, has led to the presence of severe oscillations until settling at the reference setpoint. This case is depicted in Fig. 9. Proportional gain values of less than 20 were not enough to lead to such an increase of pressure that would move the climber to the desired position. Therefore, the tests focused mainly on K_p values from 20 to 60.

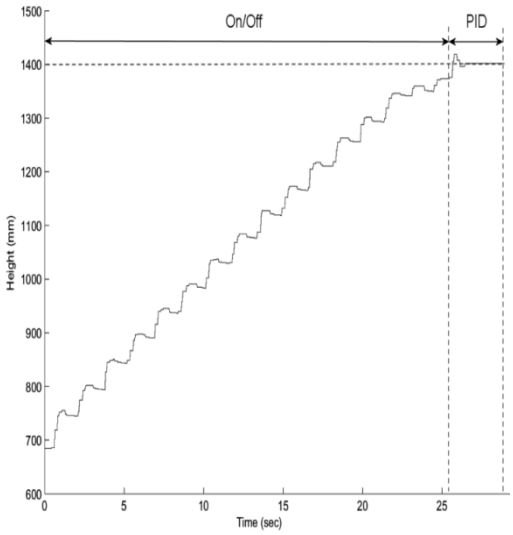

Fig. 8 Robotic climber experimental response ($r = 1400$ mm, $K_p = 40, K_i = 0.18, K_d = 0.01, Q = 20$)

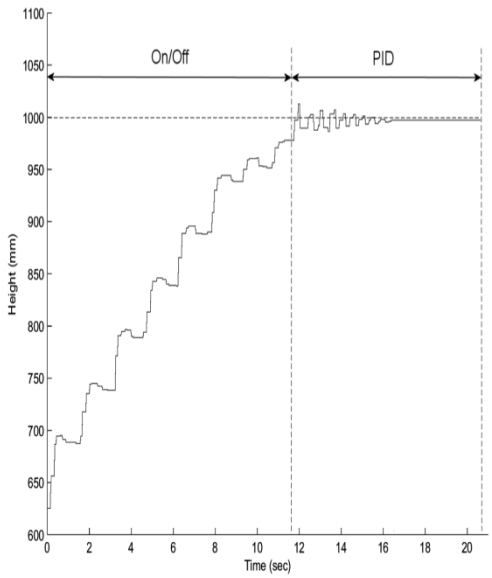

Fig. 9 Robotic climber experimental response ($r = 1000\ mm,\ K_p = 60, K_i = 0.21, K_d = 0.001, Q = 10$)

In Fig. 10 sequential snapshots during the robot climber's ascent and depict the states of the muscles during the execution of the On/Off algorithm described in the previous sections. In the first snapshot the climber is in its idle state. In the second, the lower muscles contract and then the upper muscles contract as well. The upper muscles extend in the fourth and the climber returns in its idle state in the fifth snapshot. The same sequence of muscle states repeats itself and ends with the climber in idle state as it is presented from the sixth to the ninth snapshot.

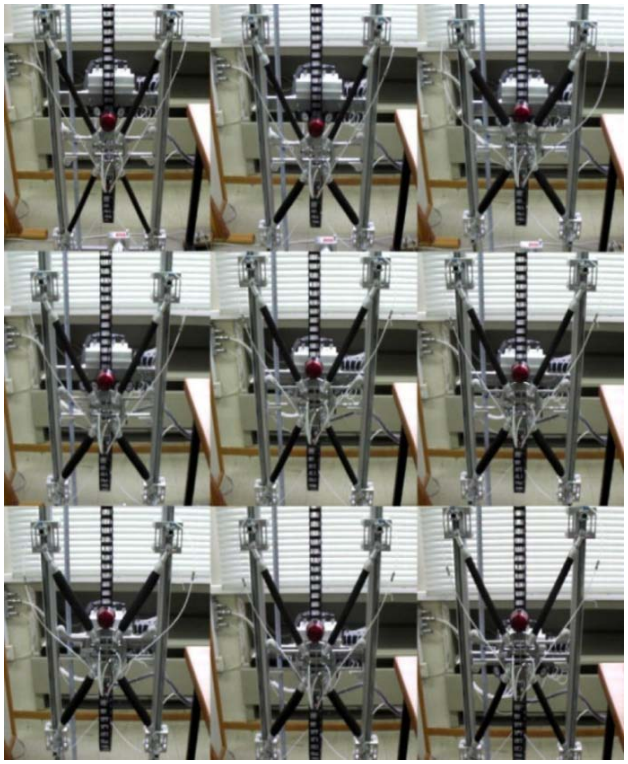

Fig. 10 Snapshots showing the climber's ascent

V. CONCLUSIONS

In this article the development and control of a novel hybrid controlled vertical climbing robot based on Pneumatic Muscle Actuators (PMAs) has been presented. The vertical sliding of the robot was based on four PMAs and through the combined and sequential contraction– extension of the pneumatic muscles and cylinders, upward and downward movements were executed. For controlling the movement of the robot and to cope with the high non–linearities of the system, a simplified and highly functional hybrid control scheme, based on PID and On/Off control, has been adopted. The efficacy of the proposed scheme is presented through multiple experimental results where it is shown that the utilized controller is able to provide fast (on/off) and accurate (PID) translations to the robot.

REFERENCES

[1] A. Degani, A. Shapiro, H.C. and M.T. Mason, (2007). "A dynamic single actuator vertical climbing robot." 2901–2906.

[2] W. M. Shen, J. Gu, and Y. J. Shen. "Proposed wall climbing robot with permanent magnetic tracks for inspecting oil tanks citation." volume 4, 2005.

[3] T. S. White, R. Alexander, R. G. Callow, A. Cooke, and J. Sargent. "A mobile climbing robot for high precision manufacture and inspection of aerostructures." International Journal of Robotics Research, 24(7):589–598, 2005.

[4] F. Rochat, P. Schoeneich, B. Luthi, F. Mondada, H. Bleuler, H. Fujimoto, M. Tokhi, H. Mochiyama, and G. Virk. "A simple and miniature climbing robot with advance mobility in ferromagnetic environment." Aug 2010.

[5] Y. Jiang, H.Wang, L. Fang, and M. Zhao. "Motion planning for climbing robot based on hybrid navigation." pages 91– 100, 2005.

[6] H. Bingshan, W. Wang, Y. Zhao, and Z. Fu. "A miniature wall climbing robot with biomechanical suction cups." Industrial Robot: An International Journal, 36(6):551–561, 2009.

[7] D. Caldwell, G. Medrano-Cerda, and M. Goodwin, "Braided pneumatic actuator control of a multi-jointed manipulator," in Proceedings of the IEEE International Conference on Systems, Man and Cybernetics, Le Touquet, 1993, pp. 423–428.

[8] V. Nickel, J. Perry, and A. Garrett, "Development of useful function in the severely paralyzed hand," Journal of Bone and Joint Surgery, vol. 45-A, no. 5, pp. 933–952, 1963.

[9] H. Schulte, "The characteristics of the McKibben Artificial Muscle," in The Application of External Power in Prosthetics and Orthotics, Lake Arrowhead, 1961, pp. 94–115.

[10] G. K. Klute and B. Hannaford, "Modeling Pneumatic McKibben Artificial Muscle Actuators: Approaches and Experimental Results," ASME Journal of Dynamic Systems, Measurements, and Control, 1999.

[11] ——,"Accounting for elastic energy storage in McKibben artificial muscle actuators," ASME Journal of Dynamic Systems, Measurement and Control, pp. 386–388, 2000.

[12] J. Yarlott, "Fluid actuator ," US Patent No. 3 645 173, 1972.

[13] D. Caldwell and N. Tsagarakis, "Biomimetic actuators in prosthetic and rehabilitation applications," Technology and Health Care, pp. 107– 120, 2002.

[14] H. DeHaven. "Tensioning device for producing a linear pull." US Patent No. 2483088, 1949.

[15] P. Desmaroux. "Improvements on tubular membranes used as a servo motor." French Patent No. 951885, 1947.

[16] R. Pierce. "Expansible cover." US Patent No. 2211478, 1940.

[17] R. H. Galyord, "Fluid Actuated Motor System and Stroking Device." US Patent no. 2,844,126, 22 July 1958.

[18] P.Warszawska. "Artificial pneumatic muscle." Dutch patent No. 6704918, 1967.

[19] B. Hannaford and J. M. Winters, "Actuator properties and movement control: biological and technological models," in Multiple Muscle Systems: Biomechanics and Movement Organization, New York, 1990, pp. 101–120.

[20] G. Andrikopoulos, G. Nikolakopoulos, and S. Manesis, "A Survey on Applications of Pneumatic Artificial Muscles", in 19th Mediterranean Conference on Control and Automation, June 20-23, Corfu, Greece, 2011.

[21] E. Kelasidi, G. Andrikopoulos, G. Nikolakopoulos, and S. Manesis, "A Survey on Pneumatic Muscle Actuators Modeling", in 20th IEEE International Symposium on Industrial Electronics (ISIE 2011), Gdansk, Poland, 2011.

[22] B. Tondu and P. Lopez. Modeling and control of mckibben artificial muscle robot actuators. IEEE Control Systems Magazine, 20(2):15–38, 2000.